

Non-Abelian Evolution of a Majorana Train in a Single Josephson Junction

Sang-Jun Choi^{1,2} and H.-S. Sim^{1,*}

¹Department of Physics, Korea Advanced Institute of Science and Technology, Daejeon 34141, Korea

²Center for Theoretical Physics of Complex Systems, Institute for Basic Science, Daejeon 34126, Korea
(Dated: April 7, 2024)

Demonstration of non-Abelian anyon statistics often requires dynamical controls of a complicated device that are challenging in realistic situations. We propose a *single* Josephson junction to detect a non-Abelian statistics effect of Majorana fermions, formed by two finite-size *s*-wave superconductors on a topological insulator under a magnetic field. At certain field strengths, a train of three localized Majorana fermions appears along the junction, while an extended chiral Majorana fermion encircles the train and the superconductors. A DC voltage bias across the junction causes the train to move and collide with the extended Majorana fermion. This involves interchange of fusion partners among the four Majorana fermions. This gives rise to non-Abelian state evolution and a $2n\pi$ fractional AC Josephson effect. The period-elongation factor n is an integer $n \geq 2$ tunable by the voltage.

When non-Abelian anyons adiabatically exchange their positions and fuse, the system can evolve from one state to another [1–5]. The non-Abelian statistics is a key of topological quantum computing where one operates qubits in a nonlocal way immune to local decoherence.

There are efforts to realize non-Abelian anyons. For example, Majorana fermions emerge in effective *p*-wave superconductors (SCs) [6–11]. Their existence is supported by observation of zero-bias conductance peaks [12–18] and fractional AC Josephson effects [19–22]. Their non-Abelian statistics, though, has not yet been detected. Related proposals utilize Josephson tri-junctions on a topological insulator [8] or nanowire junctions [23–26]. These require dynamical control of a number of electrical gates or SC phase differences in multiple junctions, and need additional setups to detect the statistics.

Fractional Josephson effects are hallmarks of topological SCs. A Majorana zero mode (MZM) allows single-electron transfer across a Josephson junction, resulting in 4π periodic current as a function of the SC phase difference of the junction [27–29]. Fractional Josephson effects of a longer period can occur when electron-electron interactions or parafermions play a role [30–35]. The present work predicts a new fractional Josephson effect originating from the non-Abelian statistics.

In this work, we propose a *single* Josephson junction to detect the non-Abelian statistics. It hosts four Majorana fermions $\gamma_{k=1,2,3,4}$'s with the help [36] of an external magnetic field (Fig. 1). Voltage bias V_{DC} across the junction makes γ_k 's move and collide each other. This involves interchange of fusion partners among γ_k 's, causing non-Abelian state evolution, such as $|00\rangle \mapsto (e^{i\phi_+}|00\rangle - ie^{i\phi_-}|11\rangle)/\sqrt{2}$, in one conventional Josephson period $T_J = h/(2eV_{DC})$. $|00\rangle$ and $|11\rangle$ are fermion occupation states formed by γ_k 's. ϕ_{\pm} 's are V_{DC} -dependent dynamical phases arising from fusion and splitting of γ_k 's. The evolution returns to the initial state after time nT_J , showing a $2n\pi$ fractional AC Josephson effect. The period-elongation factor n is an integer ≥ 2 tunable by V_{DC} . The effect can be detected by Shapiro spikes.

Setup.— Figure 1(a) shows two topological SCs induced by *s*-wave SCs on a topological insulator (TI) surface [37]. Perpendicular magnetic fields B (or Zeeman fields M by magnetic insulators), applied to the surface outside the SCs, break the time reversal symmetry, opening an energy gap at the Fermi energy. Then an extended chiral Majorana mode u (1), whose operator is $\eta_{u(1)}(x) = \eta_{u(1)}^\dagger(x)$, is formed along the boundary between the upper

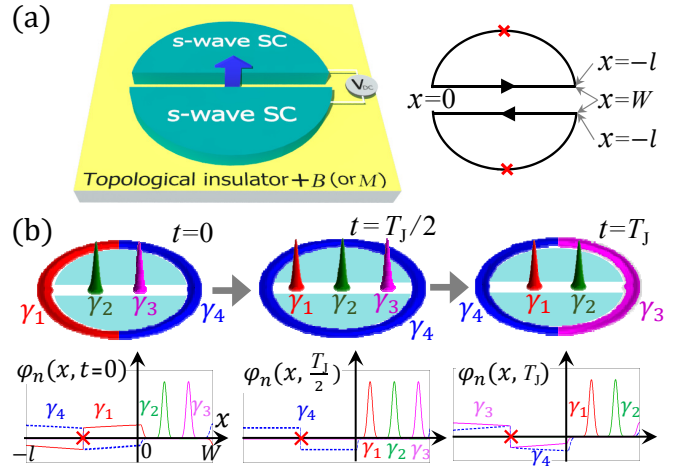


FIG. 1. (a) Topological Josephson junction under magnetic fields B . Right: Coordinate $x \in [-l, W]$ of the SC edges, along which chiral Majorana modes propagate (arrows). Crosses depict branch cuts at $x = -l/2$ on the arcs. (b) When three magnetic flux quanta (thick arrow) pierce the junction, four Majorana fermions $\gamma_{k=1,2,3,4}$ appear. Their probability distribution $|\varphi_k(x, t)|^2$ (upper panels) and wave function $\varphi_k(x, t)$ (lower) are numerically obtained. At time $t = 0$, γ_1 and γ_4 extend and overlap along the arcs, forming a fusion pair. γ_2 and γ_3 are localized MZMs in the junction and compose another fusion pair. Voltage bias V_{DC} across the junction makes γ_k 's move. At $t = T_J/2$, all γ_k 's become MZMs. At T_J , γ_3 collides with the arcs, fusing with γ_4 , while γ_1 fuses with γ_2 . The fusion partners interchange as $\{(\gamma_4, \gamma_1), (\gamma_3, \gamma_2)\}_{t=0} \rightarrow \{(\gamma_4, \gamma_3), (\gamma_2, \gamma_1)\}_{T_J}$, leading to non-Abelian state evolution.

(lower) topological SC and the gapped TI region due to topological origin [8, 38–42]. $x \in [-l, W]$ is the coordinate along the SC edge. The mode gains Berry phase π after one circulation along the edge, when each SC has no vortex. To describe this, we place a branch cut [39] at $x = -l/2$: $\eta_{u(1)}(-l/2+0^+) = -\eta_{u(1)}(-l/2-0^+)$ with positive infinitesimal 0^+ , and choose $\eta_{u(1)}(-l) = \eta_{u(1)}(W)$.

The two SCs form a short Josephson junction of length L and width W . Three magnetic flux quanta are enclosed by the junction area, $N = BLW/\Phi_0 = 3$, and e is the electron charge. The junction Hamiltonian [8, 43] is

$$H(t) = \int_{-l}^W dx \Gamma(x)^\top (-i\hbar v(x)\sigma_z \partial_x + m(x,t)\sigma_y) \Gamma(x). \quad (1)$$

$\sigma_{x,y,z}$ are Pauli matrices and $\Gamma(x)^\top \equiv (\eta_u(x), \eta_l(x))$. Inside the junction $x \in [0, W]$, the modes η_u and η_l counterpropagate with velocity $v(x) = v_J$ and couple each other with strength $m(x,t) = \Delta_0 \sin(\frac{N\pi x}{W} - \frac{eV_{DC}t}{\hbar})$. Δ_0 is the gap of the topological SCs. $m(x,t)$ depends on x and time t , since the voltage V_{DC} and the magnetic field affect the SC phase difference of the junction. Along the arcs $x \in [-l, 0]$ of the SCs, η 's propagate with velocity $v(x) = v_{arc}$ and $m(x,t) = 0$. The upper and lower arcs have the same length l for simplicity; our results are qualitatively unchanged when their lengths are different.

Majorana train.— We write the Hamiltonian as $H(t) = i \sum_{q=1,2,\dots} E_q(t) \gamma_{2q}(t) \gamma_{2q-1}(t)$, using its particle-hole symmetry. The Majorana operators $\gamma_{j=2q-1,2q}$ associated with the single-particle level E_q are found as $\gamma_j(t) = \int_{-l}^W dx [\eta_u(x) - (-1)^j \eta_l(x)] \varphi_j(x, t)$. $\varphi_j(x, t)$ is the real wave function of γ_j . We obtain the levels $E_q(t)$ in Fig. 2(a), numerically solving Eq. (1) with realistic parameters that satisfy the conditions ($\lambda \ll W/3$, $T_J \gg \hbar/E_0$) explained later. The two lowest levels have zero energy at certain times. We focus on the four Majorana fermions $\gamma_{k=1,2,3,4}$ associated with the two levels, labeling them with another index k . Figure 1(b) shows their wave functions.

Along the junction, a train of localized Majorana fermions $\gamma_k(t)$ appears at positions

$$x_{k=1,2,\dots}(t) = \frac{W}{N} \left(k - 1 + \frac{t}{T_J} \right) \in [0, W], \quad (2)$$

at which the SC phase difference is an integer multiple of π and $m(x,t)$ has sign change [36]. Because of V_{DC} the train moves with periodic position shift $x_k(T_J) = x_{k+1}(0)$. Distance between adjacent γ_k 's is $W/N = W/3$. A Majorana fermion γ_k is a localized MZM (well separated from its neighbors $\gamma_{k\pm 1}$ and the SC arcs) in a Gaussian wave function [43] with localization length $\lambda = \sqrt{\hbar v_J W / (N\pi \Delta_0)}$, when $\lambda \ll W/3, x_k, W - x_k$.

Along the arcs, extended chiral Majorana fermions occur. We find their energy E quantization condition [43],

$$2lE/(\hbar v_{arc}) + \pi + \pi(M_J + M_u + M_l) = 0, \pm 2\pi, \dots \quad (3)$$

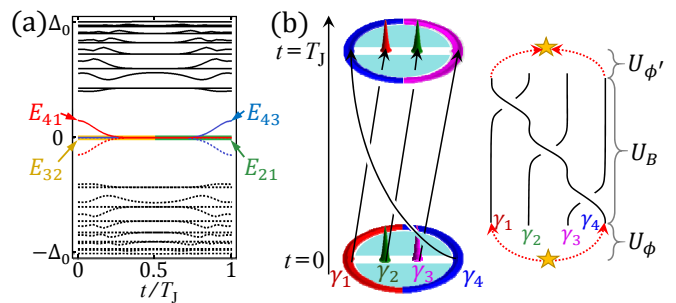


FIG. 2. (a) Numerical results of single-particle energy levels of the setup. Energy levels $E_{kk'}$ formed by the Majorana fermions $\gamma_{k=1,2,3,4}$ are marked. We choose the SC gap $\Delta_0 \sim 1$ meV (proximity-induced, e.g. by NbN SCs [44]), SC coherence length $\xi = \hbar v_F / \Delta_0 \sim 260$ nm (Fermi velocity $v_F \sim 4.0 \times 10^5$ m/s [45]), a short junction of $L \sim 60$ nm $< \xi$ and $W \sim 800$ nm, $B \sim 130$ mT ($N = 3$), $2l \sim 2.5$ μ m, $v_{arc} \sim v_F$, $v_J \sim 0.04 v_F$ [43], and $M_u = M_l = 0$. These parameters satisfy $\lambda \ll W/3$. (b) World lines equivalent to the evolution of γ_k 's during one Hamiltonian period T_J . The fusion of $\gamma_4(t)$ and $\gamma_1(t)$ in $t \in [0, T_J/2]$ and that of $\gamma_4(t)$ and $\gamma_3(t)$ in $[T_J/2, T_J]$ are depicted by stars.

The first two terms are the dynamical phase and Berry phase gained in one circulation along the upper and lower arcs of total length $2l$. $M_{u(l)}$ is the number of MZMs in vortices inside the upper (lower) SC. M_J is the number of the localized MZMs [equivalently, the number of sign changes of $m(x,t)$ in Eq. (2)] inside the junction [36]. The condition implies that an extended chiral MZM appears along the arcs, when the total number of MZMs inside the junction and the two SCs is odd. The appearance is insensitive to the details of $m(x,t)$ and the arcs. This chiral MZM was not considered in previous works [36]. We will consider the case of $M_u = M_l = 0$ [43].

Fusion-partner interchange.— When two MZMs γ_k and $\gamma_{k'}$ collide, they fuse to form fermion occupation states $|0_{kk'}\rangle_t, |1_{kk'}\rangle_t = f_{kk'}^\dagger(t) |0_{kk'}\rangle_t$. Here $f_{kk'}(t) = [\gamma_k(t) + i\gamma_{k'}(t)]/2$. As shown below, a sequence of such fusions occur in our system, resulting in non-Abelian state evolution in the adiabatic regime of $T_J \gg \hbar/E_0$ that the energy gap E_0 between the two lowest levels by γ_k 's and the other midgap levels is much larger than $2eV_{DC}$.

At $t = 0$, the Majorana fermions $\gamma_{k=1,2,3,4}$'s appear at $x = (k-1)W/3$ along the junction [see Fig. 1(b)]. γ_1 and γ_4 are localized in the junction but overlap each other along the arcs, fusing into a state $|0_{41}\rangle_{t=0}$ of energy $-E_{41}(t=0) < 0$ and $|1_{41}\rangle_{t=0}$ of $E_{41}(t=0)$. When $\lambda \ll W/3$, γ_2 and γ_3 are localized MZMs and form fusion states $|0_{32}\rangle_{t=0}$ and $|1_{32}\rangle_{t=0}$ with zero energy $E_{32} = 0$. Hence the junction has two-fold degenerate ground states, $|0_{41}0_{32}\dots\rangle_0$ and $|0_{41}1_{32}\dots\rangle_0$ [46]. We follow the time evolution of the even-parity ground state $|\psi(t=0)\rangle = |0_{41}0_{32}\rangle_0$. Here the part $|\dots\rangle_0$ for the other midgap levels is ignored, since its evolution is trivial [43].

In $t \in [0, T_J/2]$, $\gamma_{1,2,3}$'s move along the junction and

γ_4 further moves into the arcs. $\gamma_2(t)$ and $\gamma_3(t)$ remain MZMs ($E_{32} = 0$), while $\gamma_4(t)$ and $\gamma_1(t)$ become split and their energy $E_{41}(t)$ decreases with t . At $t = T_J/2$, $\gamma_{1,2,3,4}(t)$'s all become MZMs, having no overlap each other. $\gamma_4(T_J/2)$ is the extended chiral MZM along the arcs, obeying Eq. (3) at $E = 0$. Hence the low-energy part of $H(t)$ is reduced into the Hamiltonian $H_{\text{MF}}(t) = iE_{41}(t)\gamma_4(t)\gamma_1(t) = E_{41}(t)[2f_{41}^\dagger(t)f_{41}(t) - 1]$. Notice $E_{41}(T_J/2) = 0$. The initial state $|0_{41}0_{32}\rangle_0$ adiabatically evolves into $|\psi(t = T_J/2)\rangle = e^{i\phi}|0_{41}0_{32}\rangle_{T_J/2}$, gaining dynamical phase $\phi = \int_0^{T_J/2} dt' E_{41}(t')/\hbar$.

In $t \in [T_J/2, T_J]$, $\gamma_3(t)$ approaches the arcs and fuses with $\gamma_4(t)$, forming states $|0_{43}\rangle_t$ and $|1_{43}\rangle_t$ of energy $\mp E_{43}(t)$. $E_{43}(t)$ increases with t . $\gamma_1(t)$ and $\gamma_2(t)$ are MZMs, and their zero-energy fusion states are $|0_{21}\rangle_t$ and $|1_{21}\rangle_t$. Hence $H_{\text{MF}}(t) = E_{43}(t)[2f_{43}^\dagger(t)f_{43}(t) - 1]$ in this domain. The fusion-partner interchange happens as $\{(\gamma_4, \gamma_1), (\gamma_3, \gamma_2)\}_{t \in [0, T_J/2]} \rightarrow \{(\gamma_4, \gamma_3), (\gamma_2, \gamma_1)\}_{[T_J/2, T_J]}$. To find $|\psi(t)\rangle$ in $t \in [T_J/2, T_J]$, we write $|\psi(t = T_J/2)\rangle = e^{i\phi}|0_{41}0_{32}\rangle_{T_J/2}$ in terms of the new fusion states,

$$e^{i\phi}|0_{41}0_{32}\rangle_{T_J/2} = \frac{e^{i\phi}}{\sqrt{2}}(|0_{43}0_{21}\rangle_{T_J/2} + |1_{43}1_{21}\rangle_{T_J/2}), \quad (4)$$

in accord with the fusion rule $\sigma \times \sigma = I + \psi$ [1] of $\gamma_k(T_J/2)$'s. The state adiabatically evolves into $|\psi(T_J)\rangle = \frac{e^{i\phi}}{\sqrt{2}}(e^{i\phi'}|0_{43}0_{21}\rangle_{T_J} + e^{-i\phi'}|1_{43}1_{21}\rangle_{T_J})$ at $t = T_J$, as $|0_{43}0_{21}\rangle_t$ and $|1_{43}1_{21}\rangle_t$ are the eigenstates of $H_{\text{MF}}(t)$ in $t \in [T_J/2, T_J]$. The dynamical phase $\pm\phi' = \mp \int_{T_J/2}^{T_J} dt' E_{43}(t')/\hbar$ arises by the fusion of γ_3 and γ_4 .

Non-Abelian evolution.— To see the non-Abelian nature of the state evolution, we find the relations between the wave functions of γ_k 's at $t = 0$ and T_J in Fig. 1(b),

$$\varphi_{k=1,2,3}(x, T_J) = \varphi_{k+1}(x, 0), \quad \varphi_4(x, T_J) = -\varphi_1(x, 0), \quad (5)$$

The factor -1 accords with the phase gain of a Majorana vortex that exchanges positions with three other vortices, passing their branch cuts. Equivalently, $\gamma_{k=1,2,3}(T_J) = \gamma_{k+1}(0)$, $\gamma_4(T_J) = -\gamma_1(0)$, $f_{21}(T_J) = f_{32}(0)$, $f_{43}(T_J) = i f_{41}(0)$. Using this we find non-Abelian evolution $|\psi(0)\rangle \mapsto |\psi(T_J)\rangle$ in one Hamiltonian period,

$$|0_{41}0_{32}\rangle_0 \mapsto |\psi(T_J)\rangle = \frac{e^{i\phi}}{\sqrt{2}}(e^{i\phi'}|0_{41}0_{32}\rangle_0 - i e^{-i\phi'}|1_{41}1_{32}\rangle_0). \quad (6)$$

We obtain the non-Abelian evolution of general initial states, $|\psi(0)\rangle \mapsto |\psi(T_J)\rangle = U|\psi(0)\rangle$, in the $t = 0$ basis $\{|0_{41}0_{32}\rangle_0, |1_{41}1_{32}\rangle_0, |0_{41}1_{32}\rangle_0, |1_{41}0_{32}\rangle_0\}$,

$$U = \frac{1}{\sqrt{2}} \begin{pmatrix} e^{i\phi_+} & i e^{-i\phi_-} & 0 & 0 \\ -i e^{i\phi_-} & -e^{-i\phi_+} & 0 & 0 \\ 0 & 0 & -i e^{i\phi_+} & e^{-i\phi_-} \\ 0 & 0 & e^{i\phi_-} & -i e^{-i\phi_+} \end{pmatrix} = \begin{pmatrix} U_e & \mathbf{0} \\ \mathbf{0} & U_o \end{pmatrix}. \quad (7)$$

Here, $\phi_\pm = \phi \pm \phi'$. It is decomposed as $U = U_{\phi'} U_B U_\phi$,

$$U_\phi = \begin{pmatrix} e^{i\phi} & 0 & 0 & 0 \\ 0 & e^{-i\phi} & 0 & 0 \\ 0 & 0 & e^{i\phi} & 0 \\ 0 & 0 & 0 & e^{-i\phi} \end{pmatrix}, \quad U_B = \frac{1}{\sqrt{2}} \begin{pmatrix} 1 & i & 0 & 0 \\ -i & -1 & 0 & 0 \\ 0 & 0 & -i & 1 \\ 0 & 0 & 1 & -i \end{pmatrix}.$$

U_ϕ describes dynamical phase gain by the splitting of γ_k 's in $t \in [0, T_J/2]$, while $U_{\phi'}$ is due to the fusion in $[T_J/2, T_J]$. U_B describes the fusion-partner interchange, $\gamma_{k=1,2,3,4}(T_J) = U_B \gamma_k(0) U_B^\dagger$, which agrees Eq. (5). U_B is further decomposed, $U_B = U_{21} U_{32} U_{43}$, into a series of braidings $U_{ab} = [1 + \gamma_a(0)\gamma_b(0)]/\sqrt{2}$ of γ_a and γ_b . This coincides with the Ivanov's construction [47] obtained from the world lines in Fig. 2(b).

From Eq. (7) we find that the evolution $U_e|\varphi_e\rangle$ of an even-parity state $|\varphi_e\rangle$ in one Hamiltonian period T_J is described by its rotation about an axis by rotation angle $\Omega = 2 \arccos\left(\frac{\sin \phi_\pm}{\sqrt{2}}\right)$ on the Bloch sphere for pseudospins $|\uparrow\rangle \equiv |0_{41}0_{32}\rangle_0$, $|\downarrow\rangle \equiv |1_{41}1_{32}\rangle_0$. The state returns to the initial state, up to a phase factor, after nT_J . The period-elongation factor n is the smallest integer satisfying that $n\Omega$ equals a multiple of 2π . Since $\Omega \in [\frac{\pi}{2}, \frac{3\pi}{2}] \pmod{2\pi}$, we find $n \geq 2$, reflecting non-Abelian nature. n is experimentally tunable by V_{DC} , as ϕ_+ depends on V_{DC} as $\phi_+ = \pi \bar{E}/(eV_{\text{DC}})$ and the average energy change $\bar{E} = [\int_0^{T_J/2} E_{41}(t') dt' + \int_{T_J/2}^{T_J} E_{43}(t') dt']/T_J$ is V_{DC} independent. Odd-parity states have the same feature.

Figure 3(a) shows the energy $E_{\text{MF}}(t)$ of the state $|\psi(t)\rangle$. It is nT_J periodic. As an example, we explain the $n = 2$ case that happens when $\phi_+ = \pi$ (namely, $\Omega = \pi$). In $t \in [0, T_J/2]$, $E_{\text{MF}}(t) = -E_{41} < 0$ increases with time as $\gamma_4(t)$ and $\gamma_1(t)$ becomes split, and the state is in $|\psi(t)\rangle \propto |0_{41}0_{32}\rangle_t$. In $t \in [T_J/2, 3T_J/2]$, the state energy is zero, $E_{\text{MF}}(t) = 0$, although $\gamma_3(t)$ and $\gamma_4(t)$ fuse or split in this time interval. It is because the state is in an equal-probability superposition of $|0_{43}0_{21}\rangle_t$ and $|1_{43}1_{21}\rangle_t$ [see Eq. (4)]; the energy of $|0_{43}0_{21}\rangle_t$, $-E_{43}(t)$, is cancelled by that of $|1_{43}1_{21}\rangle_t$, $E_{43}(t)$. In $t \in [3T_J/2, 2T_J]$, $E_{\text{MF}}(t) = -E_{41} < 0$ decreases with time, since $\gamma_4(t)$ and $\gamma_1(t)$ becomes fused and the state is in $|\psi(t)\rangle \propto |0_{41}0_{32}\rangle_t$. At $t = 2T_J$ the state returns to the initial state. The other cases [48] in Fig. 3 are understood similarly.

$2n\pi$ Fractional AC Josephson effect.— The nT_J periodicity of the non-Abelian evolution is detected by the Josephson current of the junction. In Fig. 3(b) the current I_{MF} mediated by the state $|\psi(t)\rangle$ of the four Majorana fermions γ_k 's follows [43] $I_{\text{MF}} = V_{\text{DC}}^{-1} dE_{\text{MF}}/dt$. It has the period nT_J and fractional Josephson frequency $2eV_{\text{DC}}/(nh)$, although the Hamiltonian $H(t)$ is T_J periodic. The total Josephson current $I_J = I_{\text{MF}} + I_{\text{mid}}$ that includes the contribution I_{mid} from the other midgap states is also nT_J periodic, showing a $2n\pi$ fractional AC Josephson effect (I_J is computed in Ref. [43]); I_{mid} has the conventional period T_J . This is also found for odd-parity states.

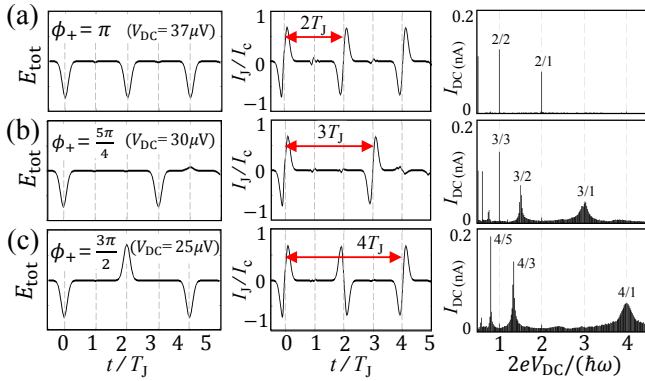


FIG. 3. $2n\pi$ fractional AC Josephson effect. For different ϕ_+ 's and V_{DC} 's, time dependence of the energy E_{MF} of $|\psi(t)\rangle$ (left panels), the Josephson current I_{MF} (normalized by its maximum I_c) mediated by $|\psi(t)\rangle$ (middle), the Shapiro spikes of long-time average of I_{MF} measured with an AC voltage of frequency ω (right). The spike positions $2eV_{\text{DC}}/(\hbar\omega)$ are represented as n/p . E_{MF} and I_{MF} have the same period nT_J , (a) $n = 2$, (b) 3, (c) 4. The numerical results are obtained with the initial state $|0_{41}0_{32}\rangle_0$ and the parameters in Fig. 2.

The current I_{MF} (or the Fourier components of I_J with period $\geq 2T_J$) carries information about the evolution of a state formed by γ_k 's. $I_{\text{MF}} \neq 0$ implies that the state gains or losses energy by fusion or splitting of γ_k 's. When $I_{\text{MF}} = 0$ in a time interval, γ_k 's are MZMs or the state is in an equal-probability superposition of two temporal eigenstates of $H_{\text{MF}}(t)$ having the same parity (such as $|0_{43}0_{21}\rangle_t$ and $|1_{43}1_{21}\rangle_t$); the two eigenstates are particle-hole symmetry partners, mediating the equal amount of current in the opposite direction.

The period-elongation factor $n \geq 2$ is tuned by the voltage V_{DC} , since the state evolution depends on the dynamical-phase gain ϕ_{\pm} by fusion and splitting of γ_k 's. This unique feature of our $2n\pi$ effect, the dependence of n on V_{DC} , is absent in the known fractional Josephson effects [30–35]. It can be observed in time-resolved detection of the Josephson current I_J .

This can be also seen by measuring Shapiro spikes with applying an AC voltage $V(t) = V_{\text{DC}} + V_{\text{AC}} \sin(\omega t)$ of frequency ω across the junction. For $2eV_{\text{AC}} \ll \min\{2eV_{\text{DC}}, \hbar\omega\}$, where the state evolution is affected weakly by V_{AC} , we numerically compute the evolution of the initial state $|0_{41}0_{32}\rangle_0$ and the average of the Josephson current mediated by the state over a long time $\sim 10^4 T_J$ (Fig. 3). The average shows a peak (Shapiro spike) when $2eV_{\text{DC}} = (qn/p)\hbar\omega$ is satisfied with $q = 1, 2, \dots$ and certain integers $p \geq 1$. Only the spikes of $q = 1$ are visible at $2eV_{\text{AC}} \ll \hbar\omega$, as the spike heights $\propto (\frac{2eV_{\text{AC}}}{\hbar\omega})^q$ [49]. A spike at $2eV_{\text{DC}}/(\hbar\omega) = n/p$ implies the Fourier components p of the nT_J -periodic supercurrent $I_{\text{MF}}(t)$ at $V_{\text{AC}} = 0$, expressed as $I_{\text{MF}}(t) = \sum_{p=1}^{\infty} a_p \sin \frac{2\pi pt}{nT_J}$; the spike height is proportional to a_p . For example, in the $n = 2, 3$ cases of Fig. 3(a,b), the spikes appear at

$2eV_{\text{DC}}/(\hbar\omega) = n/1, n/2, \dots$. In the $n = 4$ case, the spikes appear at $2eV_{\text{DC}}/(\hbar\omega) = n/p = 4/1, 4/3, 4/5, \dots$, since $I_{\text{MF}}(t)$ does not have even- p components in Fig. 3(c) ($a_2 = a_4 = \dots = 0$). The $p \geq 2$ (high harmonics) components reflect the nonsinusoidal supercurrent resulting from the fusion and splitting of γ_k 's. The spike positions are different from the case of conventional 2π currents where a visible spike occurs only at $2eV_{\text{DC}}/(\hbar\omega) = 1$ for $2eV_{\text{AC}} \ll \hbar\omega$ (or at $1, 2, 3, \dots$ for larger V_{AC}). Notably, the sequence of the spike positions n/p depends on V_{DC} in our $2n\pi$ current. Detection of these features are within reach, as the Shapiro steps for 4π supercurrents have been observed [19–22]. Spikes at larger V_{AC} is studied in Ref. [43].

Discussion.— To have the non-Abelian evolution, the adiabatic regime $T_J \gg \hbar/E_0$ is required. We estimate [43] $\hbar/E_0 \sim 0.004$ ns, based on the minimum excitation energy $E_0 \sim \pi\hbar v_{\text{arc}}/(2l)$ of the setup with $2l \sim 2.5 \mu\text{m}$ and $v_{\text{arc}} \sim v_F$. The regime is satisfied by $T_J = 0.03 \sim 0.08$ ns (equivalently, $V_{\text{DC}} = 25 \sim 74 \mu\text{V}$ and $\phi_+ = \pi/2 \sim 3\pi/2$). This time scale is shorter than $\hbar/k_B T \sim 0.16$ ns at temperature $T = 50$ mK and quasi-particle poisoning time $0.1 \sim 1 \mu\text{s}$ [50]. The parameters in Fig. 2 satisfy $W > \xi$, with which γ_k 's form “nonlocal” electrons spatially separated by distance ($\sim W$) larger than ξ , suppressing state flip $|0_{41}0_{32}\rangle_0 \leftrightarrow |1_{41}1_{32}\rangle_0$ by Cooper-pair transfer between γ_k 's and the SCs.

According to our numerical study [43], the $2n\pi$ supercurrent I_{MF} is comparable with the 2π supercurrent I_{mid} by the midgap states, and the total current $I_J = I_{\text{MF}} + I_{\text{mid}}$ shows the $2n\pi$ features of the Shapiro spikes in Fig. 3; I_{mid} leads to only one additional spike at $2eV_{\text{DC}}/(\hbar\omega) = 1$. The $2n\pi$ fractional AC Josephson effect does not require fine tuning of the magnetic flux, V_{DC} , and the chemical potential of the TI [43]. It also occurs, with modifications, in the presence of vortices in the SCs ($M_{a=u,1} \neq 0$) [43]. Our proposal is realizable with various effective p -wave SCs [51–61].

In summary, the $2n\pi$ fractional AC Josephson effect, a signature of the non-Abelian statistics, can occur in a *single* Josephson junction, a setup much simpler than the existing proposals. The junction can be used to demonstrate other non-Abelian statistics effects such as the non-commutativity of non-Abelian evolution U 's [43].

We thank Myung-Ho Bae, Sungjae Cho, Gleb Finkelstein, David Goldhaber-Gordon, Gil-Ho Lee, Bernard Plaças, Felix von Oppen, Yuval Oreg, Leonid Rokhinson, Ady Stern, and Björn Trauzettel for valuable discussions. We are supported by Korea NRF (Grant No. 2016R1A5A1008184).

* Corresponding author.hssim@kaist.ac.kr

[1] C. Nayak, S. H. Simon, A. Stern, M. Freedman, and S.

- D. Sarma, Non-Abelian anyons and topological quantum computation, *Rev. Mod. Phys.* **80**, 1083 (2008).
- [2] A. Stern, Non-Abelian states of matter, *Nature* **464** 187 (2010).
- [3] J. Alicea, New directions in the pursuit of Majorana fermions in solid state systems, *Rep. Prog. Phys.* **75**, 076501 (2012).
- [4] M. Leijnse and K. Flensberg, Introduction to topological superconductivity and Majorana fermions, *Semicond. Sci. Technol.* **27**, 124003 (2012).
- [5] R. Aguado, Majorana quasiparticles in condensed matter, *Riv. Nuovo Cimento* **40**, 523 (2017).
- [6] R. M. Lutchyn, J. D. Sau, and S. Das Sarma, Majorana Fermions and a Topological Phase Transition in Semiconductor-Superconductor Heterostructures, *Phys. Rev. Lett.* **105**, 077001 (2010).
- [7] Y. Oreg, G. Refael, and F. von Oppen, Helical Liquids and Majorana Bound States in Quantum Wires, *Phys. Rev. Lett.* **105**, 177002 (2010).
- [8] L. Fu and C. L. Kane, Superconducting Proximity Effect and Majorana Fermions at the Surface of a Topological Insulator, *Phys. Rev. Lett.* **100**, 096407 (2008).
- [9] S. Nadj-Perge, I. K. Drozdov, B. A. Bernevig, and A. Yazdani, Proposal for realizing Majorana fermions in chains of magnetic atoms on a superconductor, *Phys. Rev. B* **88**, 020407 (2013); J. Klinovaja, P. Stano, A. Yazdani, and D. Loss, Topological Superconductivity and Majorana Fermions in RKKY Systems, *Phys. Rev. Lett.* **111**, 186805 (2013)
- [10] Xiao-Liang Qi, Taylor L. Hughes, and Shou-Cheng Zhang, Chiral topological superconductor from the quantum Hall state, *Phys. Rev. B* **82**, 184516 (2010).
- [11] Roger S. K. Mong, David J. Clarke, Jason Alicea, Netanel H. Lindner, Paul Fendley, Chetan Nayak, Yuval Oreg, Ady Stern, Erez Berg, Kirill Shtengel, and Matthew P. A. Fisher, Universal topological quantum computation from a superconductor/Abelian quantum Hall heterostructure, *Phys. Rev. X* **4**, 011036 (2014).
- [12] V. Mourik, K. Zuo, S. M. Frolov, S. R. Plissard, E. P. A. M. Bakkers, and L. P. Kouwenhoven, Signatures of Majorana Fermions in Hybrid Superconductor-Semiconductor Nanowire Devices, *Science* **336**, 1003 (2012).
- [13] A. Das, Y. Ronen, Y. Most, Y. Oreg, M. Heiblum, and H. Shtrikman, Zero-bias peaks and splitting in an AlNAs nanowire topological superconductor as a signature of Majorana fermions, *Nat. Phys.* **8**, 887 (2012).
- [14] M. T. Deng, C. L. Yu, G. Y. Huang, M. Larsson, P. Caroff, and H. Q. Xu, Anomalous Zero-Bias Conductance Peak in a NbInSb Nanowire/Nb Hybrid Device, *Nano Lett.* **12**, 6414 (2012).
- [15] S. Nadj-Perge, I. K. Drozdov, Jian Li, Hua Chen, Sangjun Jeon, Jungpil Seo, A. H. MacDonald, B. A. Bernevig, and A. Yazdani, Observation of Majorana fermions in ferromagnetic atomic chains on a superconductor, *Science* **346**, 602 (2014).
- [16] Jin-Peng Xu, Mei-Xiao Wang, Zhi Long Liu, Jian-Feng Ge, Xiaojun Yang, Canhua Liu, Zhu An Xu, Dandan Guan, Chun Lei Gao, Dong Qian, Ying Liu, Qiang-Hua Wang, Fu-Chun Zhang, Qi-Kun Xue, and Jin-Feng Jia, Experimental Detection of a Majorana Mode in the core of a Magnetic Vortex inside a Topological Insulator-Superconductor $\text{Bi}_2\text{Te}_3/\text{NbSe}_2$ Heterostructure, *Phys. Rev. Lett.* **114**, 017001 (2015).
- [17] Hao-Hua Sun, Kai-Wen Zhang, Lun-Hui Hu, Chuang Li, Guan-Yong Wang, Hai-Yang Ma, Zhu-An Xu, Chun-Lei Gao, Dan-Dan Guan, Yao-Yi Li, Canhua Liu, Dong Qian, Yi Zhou, Liang Fu, Shao-Chun Li, Fu-Chun Zhang, and Jin-Feng Jia, Majorana Zero Mode Detected with Spin Selective Andreev Reflection in the Vortex of a Topological Superconductor, *Phys. Rev. Lett.* **116**, 257003 (2016).
- [18] Hao Zhang, Chun-Xiao Liu, Sasa Gazibegovic, Di Xu, John A. Logan, Guanzhong Wang, Nick van Loo, Jouri D. S. Bommer, Michiel W. A. de Moor, Diana Car, Roy L. M. Op het Veld, Petrus J. van Veldhoven, Sebastian Koelling, Marcel A. Verheijen, Mihir Pendharkar, Daniel J. Pennachio, Borzoyeh Shojaei, Joon Sue Lee, Chris J. Palmstrøm, Erik P. A. M. Bakkers, S. Das Sarma, and Leo P. Kouwenhoven, Quantized Majorana conductance, *Nature* **556**, 74 (2018).
- [19] L. P. Rokhinson, X. Liu, and J. K. Furdyna, The fractional a.c. Josephson effect in a semiconductor superconductor nanowire as a signature of Majorana particles, *Nat. Phys.* **8**, 795 (2012).
- [20] J. Wiedenmann, E. Bocquillon, R.S. Deacon, S. Hartinger, O. Herrmann, T.M. Klapwijk, L. Maier, C. Ames, C. Brüne, C. Gould, A. Oiwa, K. Ishibashi, S. Tarucha, H. Buhmann, and L.W. Molenkamp, 4π -periodic Josephson supercurrent in HgTe-based topological Josephson junctions, *Nat. Commun.* **7**, 10303 (2016).
- [21] R. S. Deacon, J. Wiedenmann, E. Bocquillon, F. Dominguez, T. M. Klapwijk, P. Leubner, C. Brüne, E. M. Hankiewicz, S. Tarucha, K. Ishibashi, H. Buhmann, and L.W. Molenkamp, Josephson Radiation from Gapless Andreev Bound States in HgTe-Based Topological Junctions, *Phys. Rev. X* **7**, 021011 (2017).
- [22] Dominique Laroche, Danil Bouman, David J. van Wierkom, Alex Proutski, Chaitanya Murthy, Dmitry I. Pikulin, Chetan Nayak, Ruben J.J. van Gulik, Jesper Nygård, Peter Krogstrup, Leo P. Kouwenhoven, and Attila Geresdi, Observation of the 4π -periodic Josephson effect in indium arsenide nanowires, *Nat. Commun.* **10**, 245 (2019).
- [23] J. Alicea, Y. Oreg, G. Refael, F. von Oppen, and Matthew P. A. Fisher, Non-Abelian statistics and topological quantum information processing in 1D wire networks, *Nat. Phys.* **7**, 412 (2011).
- [24] D. Aasen, M. Hell, R. V. Mishmash, A. Higginbotham, J. Danon, M. Leijnse, T. S. Jespersen, J. A. Folk, C. M. Marcus, K. Flensberg, and J. Alicea, Milestones Toward Majorana-Based Quantum Computing, *Phys. Rev. X* **6**, 031016 (2016).
- [25] B. van Heck, A. R. Akhmerov, F. Hassler, M. Burrello, and C.W.J. Beenakker, Coulomb-assisted braiding of Majorana fermions in a Josephson junction array, *New J. Phys.* **14**, 035019 (2012).
- [26] T. Hyart T, B. van Heck, I. C. Fulga, M. Burrello, A. R. Akhmerov, and C.W.J. Beenakker, Flux-controlled quantum computation with Majorana fermions, *Phys. Rev. B* **88**, 035121 (2013).
- [27] A. Y. Kitaev, Unpaired Majorana fermions in quantum wires, *Phys. Usp.* **44**, 131 (2001).
- [28] H.-J. Kwon, K. Sengupta, and V. M. Yakovenko, Fractional ac Josephson effect in p - and d -wave superconductors *Euro. Phys. J. B* **37**, 349 (2004).
- [29] L. Fu and C. L. Kane, Josephson current and noise at a superconductor/quantum-spin-Hall-insulator/ superconductor junction, *Phys. Rev. B* **79**, 161408 (2009).
- [30] D. J. Clarke, J. Alicea, and K. Shtengel, Exotic non-

- Abelian anyons from conventional fractional quantum Hall states, Nat. Comm. **4**, 1348 (2013).
- [31] F. Zhang and C.L. Kane, Time-Reversal-Invariant Z_4 Fractional Josephson Effect, Phys. Rev. Lett. **113**, 036401 (2014).
- [32] C. P. Orth, R. P. Tiwari, T. Meng, and T. L. Schmidt, Non-Abelian parafermions in time-reversal-invariant interacting helical systems, Phys. Rev. B **91**, 081406(R) (2015).
- [33] J. Klinovaja and D. Loss, Fractional charge and spin states in topological insulator constrictions, Phys. Rev. B **92**, 121410(R) (2015).
- [34] Y. Peng, Y. Vinkler-Aviv, P. W. Brouwer, L. I. Glazman, and F. von Oppen, Parity Anomaly and Spin Transmutation in Quantum Spin Hall Josephson Junctions Phys. Rev. Lett. **117**, 267001 (2016).
- [35] A. Zazunov, F. Buccheri, P. Sodano, and R. Egger, 6π Josephson Effect in Majorana Box Device, Phys. Rev. Lett. **118**, 057001 (2017).
- [36] Previous works studied two localized Majorana fermions in a magnetic field, which however cannot generate non-Abelian state evolution. See E. Grosfeld and A. Stern, Observing Majorana bound states of Josephson vortices in topological superconductors, Proc. Natl. Acad. Sci. U.S.A. **108**, 11810 (2011); Andrew C. Potter and L. Fu, Anomalous supercurrent from Majorana states in topological insulator Josephson junctions, Phys. Rev. B **88**, 121109(R) (2013); Sunghun Park and Patrik Recher, Detecting the Exchange Phase of Majorana Bound States in a Corbino Geometry Topological Josephson Junction, Phys. Rev. Lett. **115**, 246403 (2015).
- [37] J. R. Williams, A. J. Bestwick, P. Gallagher, Seung Sae Hong, Y. Cui, Andrew S. Bleich, J. G. Analytis, I. R. Fisher, and D. Goldhaber-Gordon, Unconventional Josephson Effect in Hybrid Superconductor-Topological Insulator Devices, Phys. Rev. Lett. **109**, 056803 (2012).
- [38] Rakesh P. Tiwari, U. Zülicke, and C. Bruder, Majorana Fermions from Landau Quantization in a Superconductor and Topological-Insulator Hybrid Structure, Phys. Rev. Lett. **110**, 186805 (2013).
- [39] Sunghun Park, Joel E. Moore, and H.-S. Sim, Absence of the Aharonov-Bohm effect of chiral Majorana fermion edge states, Phys. Rev. B **89**, 161408(R) (2014).
- [40] L. Fu and C. L. Kane, Probing Neutral Majorana Fermion Edge Modes with Charge Transport, Phys. Rev. Lett. **102**, 216403 (2009).
- [41] A. R. Akhmerov, Johan Nilsson, and C. W. J. Beenakker, Electrically Detected Interferometry of Majorana Fermions in a Topological Insulator, Phys. Rev. Lett. **102**, 216404 (2009).
- [42] K. T. Law, Patrick A. Lee, and T. K. Ng, Majorana Fermion Induced Resonant Andreev Reflection, Phys. Rev. Lett. **103**, 237001 (2009).
- [43] More general cases and the effects of the midgap states are studied in Sang-Jun Choi and H.-S. Sim, Josephson junction of finite-size superconductors on a topological insulator under a magnetic field, preprint (2019).
- [44] S.-Z. Lin, O. Ayala-Valenzuela, R. D. McDonald, L. N. Bulaevskii, T. G. Holesinger, F. Ronning, N. R. Weisse-Bernstein, T. L. Williamson, A. H. Mueller, M. A. Hoffbauer, M. W. Rabin, and M. J. Graf, Characterization of the thin-film NbN superconductor for single-photon detection by transport measurements, Phys. Rev. B **87**, 184507 (2013).
- [45] Dong-Xia Qu, Y. S. Hor, Jun Xiong, R. J. Cava, N. P. Ong, Quantum Oscillations and Hall Anomaly of Surface States in the Topological Insulator Bi_2Te_3 , Science **329**, 821 (2010).
- [46] $|0_{k_1 k_2} 0_{k_3 k_4}\rangle_t$ satisfies $f_{k_1 k_2}^\dagger(t)|0_{k_1 k_2} 0_{k_3 k_4}\rangle_t = |1_{k_1 k_2} 0_{k_3 k_4}\rangle_t$, $f_{k_3 k_4}^\dagger(t)|0_{k_1 k_2} 0_{k_3 k_4}\rangle_t = |0_{k_1 k_2} 1_{k_3 k_4}\rangle_t$, $f_{k_1 k_2}^\dagger(t)f_{k_3 k_4}^\dagger(t)|0_{k_1 k_2} 0_{k_3 k_4}\rangle_t = |1_{k_1 k_2} 1_{k_3 k_4}\rangle_t$, and $f_{k_1 k_2}(t)|0_{k_1 k_2} 0_{k_3 k_4}\rangle_t = f_{k_3 k_4}(t)|0_{k_1 k_2} 0_{k_3 k_4}\rangle_t = 0$.
- [47] D.A. Ivanov, Non-Abelian Statistics of Half-Quantum Vortices in p -Wave Superconductors, Phys. Rev. Lett. **86**, 268 (2001).
- [48] The state evolution is $2T_J$ periodic at $\phi_+ = \pi$ [Fig. 3(a)] as $|0_{41}0_{32}\rangle_0 \xrightarrow{U} (|0_{41}0_{32}\rangle_0 + ie^{i\phi_-}|1_{41}1_{32}\rangle_0)/\sqrt{2} \xrightarrow{U} |0_{41}0_{32}\rangle_0$. It is $3T_J$ periodic at $\phi_+ = 5\pi/4$ [Fig. 3(b)], $|0_{41}0_{32}\rangle_0 \xrightarrow{U} (e^{i\pi/4}|0_{41}0_{32}\rangle_0 + ie^{i\phi_-}|1_{41}1_{32}\rangle_0)/\sqrt{2} \xrightarrow{U} (e^{i\pi/4}|0_{41}0_{32}\rangle_0 - e^{i\phi_-}|1_{41}1_{32}\rangle_0)/\sqrt{2} \xrightarrow{U} |0_{41}0_{32}\rangle_0$. It is $4T_J$ periodic at $\phi_+ = 3\pi/2$ [Fig. 3(c)], $|0_{41}0_{32}\rangle_0 \xrightarrow{U} (|0_{41}0_{32}\rangle_0 + e^{i\phi_-}|1_{41}1_{32}\rangle_0)/\sqrt{2} \xrightarrow{U} |1_{41}1_{32}\rangle_0 \xrightarrow{U} (|0_{41}0_{32}\rangle_0 - e^{i\phi_-}|1_{41}1_{32}\rangle_0)/\sqrt{2} \xrightarrow{U} |0_{41}0_{32}\rangle_0$.
- [49] M. Tinkham, *Introduction To Superconductivity*, 2nd ed. (McGraw-Hill, New York, 1995).
- [50] D. Rainis and D. Loss, Majorana qubit decoherence by quasiparticle poisoning, Phys. Rev. B **85**, 174533 (2012).
- [51] Sophie Charpentier, Luca Galletti, Gunta Kunakova, Riccardo Arpaia, Yuxin Song, Reza Baghdadi, Shu Min Wang, Alexei Kalaboukhov, Eva Olsson, Francesco Tafuri, Dmitry Golubev, Jacob Linder, Thilo Bauch, and Floriana Lombard, Induced unconventional superconductivity on the surface states of Bi_2Te_3 topological insulator, Nat. Commun. **8**, 2019 (2017).
- [52] C. Kurter, A.D.K. Finck, Y. S. Hor, and D. J. Van Harlingen, Evidence for an anomalous current-phase relation in topological insulator Josephson junctions, Nat. Commun. **6**, 7130 (2015).
- [53] Antonio Fornieri, Alexander M. Whiticar, F. Setiawan, Elas Portols Marn, Asbjørn C. C. Drachmann, Anna Kesselman, Sergei Gronin, Candice Thomas, Tian Wang, Ray Kallaher, Geoffrey C. Gardner, Erez Berg, Michael J. Manfra, Ady Stern, Charles M. Marcus, Fabrizio Nichele, Evidence of topological superconductivity in planar Josephson junctions, arXiv:1809.03037.
- [54] Hechen Ren, Falko Pientka, Sean Hart, Andrew Pierce, Michael Kosowsky, Lukas Lunczer, Raimund Schlereth, Benedikt Scharf, Ewelina M. Hankiewicz, Laurens W. Molenkamp, Bertrand I. Halperin, Amir Yacoby, Topological Superconductivity in a Phase-Controlled Josephson Junction, arXiv:1809.03076.
- [55] Qing Lin He, Lei Pan1, Alexander L. Stern, Edward C. Burks, Xiaoyu Che, Gen Yin, Jing Wang, Biao Lian, Quan Zhou, Eun Sang Choi, Koichi Murata, Xufeng Kou, Zhijie Chen, Tianxiao Nie, Qiming Shao, Yabin Fan, Shou-Cheng Zhang, Kai Liu, Jing Xia, Kang L. Wang, Chiral Majorana fermion modes in a quantum anomalous Hall insulatorsuperconductor structure, Science **357**, 294 (2017).
- [56] Joel Röntynen and Teemu Ojanen, Topological Superconductivity and High Chern Numbers in 2D Ferromagnetic Shiba Lattices, Phys. Rev. Lett. **114**, 236803 (2015).
- [57] J. Li, T. Neupert, Z. Wang, A. H. MacDonald, A. Yazdani, and B. A. Bernevig, Two-dimensional chiral topo-

- logical superconductivity in Shiba lattices, *Nat. Commun.* **7**, 12297 (2016).
- [58] G. Sharma and S. Tewari, Yu-Shiba-Rusinov states and topological superconductivity in Ising paired superconductors, *Phys. Rev. B* **94**, 094515 (2016).
- [59] Y.-T. Hsu, A. Vaezi, M. H. Fischer, E.-A. Kim, Topological superconductivity in monolayer transition metal dichalcogenides, *Nat. Commun.* **8**, 14985 (2017).
- [60] M. Sato and S. Fujimoto, Topological phases of noncentrosymmetric superconductors: Edge states, Majorana fermions, and non-Abelian statistics, *Phys. Rev. B* **79**, 094504 (2009).
- [61] N. Hao and S.-Q. Shen, Topological superconducting states in monolayer FeSe/SrTiO₃, *Phys. Rev. B* **92**, 165104 (2015).
- [62] D. J. Clarke and Kirill Shtengel, Improved phase-gate reliability in systems with neutral Ising anyons, *Phys. Rev. B* **82**, 180519(R) (2010).